Three-dimensional simulation of a molten carbonate fuel cell stack using computational fluid dynamics technique

W. He [a], Q. Chen [b]

[a] *Faculty of Mechanical Engineering and Marine Technology, Delft University of Technology, 2628 CD Delft, Netherlands*
[b] *Department of Architecture, Massachusetts Institute of Technology, Cambridge, MA 02139, USA*

Abstract

The performance of a molten carbonate fuel cell stack with regard to safe and efficient electricity generation has been investigated using the computational fluid dynamics (CFD) technique. A numerical model is developed, and it is employed to calculate the three-dimensional distributions of the crucial parameters (e.g., temperature, pressure, concentration, and density) across a stack. In particular, the model can consider simultaneously the dominant processes of a stack, such as mass transport, chemical reactions, heat transfer, and the voltage–current relations. Moreover, it is also capable of calculating the mass distribution across the stack rather than assuming a uniform distribution. In this paper, the model is demonstrated by applying it to calculate fuel cells with three different manifolds (e.g., co-, counter- and cross-flow) in a stack. The model is an effective numerical tool for optimal design and operational analysis of fuel-cell stacks, e.g. for comparing performance with different manifolds and to identify operational characteristics.

Keywords: Molten carbonate fuel cells; Computational fluid dynamics

1. Introduction

Most experimental investigations of fuel cells are expensive. In addition, they can only be carried out on a small scale, with a few designs and with difficulties of measurement, e.g., of the electrical resistance. On the other hand, the cost of numerical modelling of fuel cells is low, and it is easy to set up a number of alternative new designs. With a model, the quantitative prediction of the overall performance of fuel cells can be made over a wide range of operations and for different transient conditions. Hence, the numerical simulation of fuel cells is worthwhile and has been used extensively [1].

The numerical simulation can be appropriately divided into modelling at the electrode level (micromodelling), at cell level, and at stack level (macromodelling). Micromodelling aims at building better electrodes through study of microscopic processes. However, macromodelling aims at optimizing design alternatives and determining operational strategies, provided that the electrochemical performance of the given electrodes and electrolytes are known. In this paper, macromodelling of fuel cells is emphasized. In addition, Dutch fuel-cell research and demonstration programs have a special interest in the molten carbonate fuel

cells (MCFC) [2]. Thus, this paper is exclusively aimed at MCFC modelling. Without further specification, the term 'fuel cell' refers to 'MCFC' throughout the paper.

In macromodelling of the MCFC, the two-dimensional numerical model developed by Wolf and Wilemski [3] is one of the most sophisticated fuel-cell models at the cell level. However, there are still few models at the stack level, and an equivalent cell is normally used to represent stack performance. In the parallel field of macromodelling of the solid oxide fuel cell (SOFC), the latest stack model introduced by Achenbach [4] has considered the three-dimensional current and temperature distribution across the stack, but it is still based on the assumption of a uniform mass distribution along the stack direction.

On the other hand, experimental results recently reported by Takashima [5] have indicated that there is a significant inhomogeneity (e.g. mass flow rate) along the direction of the stack, and it increases with stack height and operating pressure. This indicates that using a two-dimensional cell model to represent the stack or assuming uniform mass distribution along the stack direction is no longer appropriate for high stacks or for stacks operating at high pressure.

Therefore, an effective stack model for MCFC should be able to deal with the physical and chemical phe-

nomena across the stack, and capable of calculating the mass distribution along the stack direction. Corresponding to these requirements, development of a three-dimensional simulation model is required to take account for these effects. In this paper, the computational fluid dynamics (CFD) technique is introduced for the stack modelling. More specifically, the commercial CFD package PHOENICS [6] is implemented with formulations which describe the physical and chemical processes in a cell. The stationary results, such as the three-dimensional distributions of temperature, pressure, density and gas composition across the cell or stack, are presented as examples of the model applications. Further validation of this model and the study of the dynamic performances with regard to load-following mode will be continued.

2. Description of main processes

Fuel cells convert chemical energy directly into electrical energy. The principle of MCFC operation is shown in Fig. 1. The process involves the oxidation of a fuel (such as hydrogen) and the reduction of an oxidant (usually oxygen). Electrons pass from the fuel electrode to the oxidant electrode via an external load, and the electrical circuit is completed by ionized particles crossing an electrolyte. The main processes, which determine the fuel-cell stack performance with regard to electricity generation, are identified as mass transport, chemical, heat-transfer processes, and voltage–current relations. These are discussed in detail as follows.

2.1. Mass-transport processes

The reactant gases, fuel and gas mixture of air and CO_2, are separately fed to the anode and cathode manifolds in the fuel-cell stack. At the anode and cathode inlet manifolds, the gases are transported along the stacking direction. Further, in the cell anode and cathode flow paths, the gases flow from inlet manifold
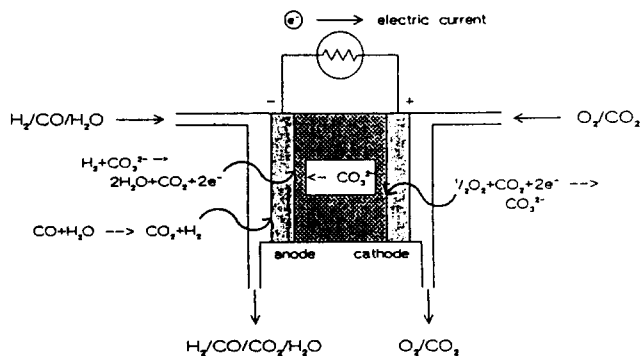

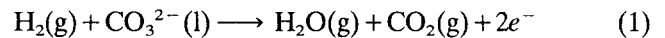Fig. 1. Electricity generation principle of MCFC.

to outlet manifold. At the anode and cathode outlet manifolds, the gases exit along the stacking direction. In the fuel cell flow path at the cell level, absorbed CO_2 and O_2 on the cathode side react to form CO_3^{2-}, which reacts at the anode side with absorbed H_2 to form H_2O and CO_2, with release of electrons.
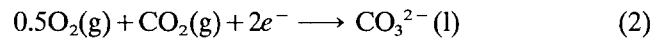
2.2. Chemical processes

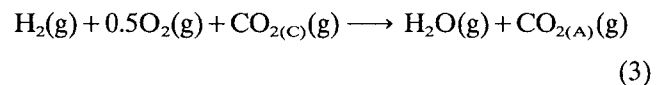The electrochemical reactions considered at the fuel-cell electrodes are the following:
(i) at the anode:

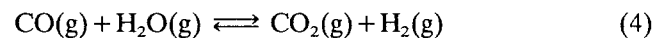$$H_2(g) + CO_3^{2-}(l) \longrightarrow H_2O(g) + CO_2(g) + 2e^- \qquad (1)$$

(ii) at the cathode:

$$0.5O_2(g) + CO_2(g) + 2e^- \longrightarrow CO_3^{2-}(l) \qquad (2)$$

The overall cell reaction is:

$$H_2(g) + 0.5O_2(g) + CO_{2(C)}(g) \longrightarrow H_2O(g) + CO_{2(A)}(g) \qquad (3)$$

where the subscripts C and A corresponds to cathode and anode, respectively.

On the anode side, also the water-shift reaction occurs, increasing the H_2 concentration:

$$CO(g) + H_2O(g) \rightleftharpoons CO_2(g) + H_2(g) \qquad (4)$$

2.3. Voltage–current relation

The maximum electrical work obtainable (W_{el}) in a fuel cell operating at constant temperature and pressure is given by the change of the Gibbs free energy (ΔG) of the electrochemical reaction:

$$W_{el} = \Delta G = -nFE \qquad (5)$$

The maximum electrical voltage obtainable (E) in a single fuel cell, which is often called reversible cell potential, is given by the Nernst equation:

$$E = E^0 + \frac{RT}{2F} \ln \frac{y_{H_2} y_{O_2}^{1/2} y_{CO_2(C)}}{y_{H_2O} y_{CO_2(A)}} + \frac{RT}{4F} \ln P \qquad (6)$$

For the overall cell reaction, the cell potential increases with an increase in the activity of reactants and a decrease in the activity of products. Changes in temperature also influence the reversible cell potential.

However, the working voltage (V) for a fuel cell is much lower than the Nernst potential. There are irreversible losses in a practical fuel cell, which primarily result from:

$$V = E - \Delta V_{diff(g)} - \Delta V_{conc} - \Delta V_{kine} - \Delta V_{diff(l)} - \Delta V_{cond} \qquad (7)$$

where $\Delta V_{diff(g)}$ is the gas diffusion, ΔV_{cond} the electronic conductivity, ΔV_{kine} the electrode kinetics, $\Delta V_{diff(l)}$ the

liquid-phase diffusion, and ΔV_{cond} the finite ionic conductivity.

At the stack modelling level, there are additional sources of loss (e.g. inhomogeneous gas flow distribution among the cells). In the present fuel cell model, the overpotential phenomena are simply considered as a voltage–current relation.

2.4. Heat-transfer processes

The heat generation in a fuel cell is a measure of its inefficiency, but it is also very important for applications such as cogeneration. It is helpful to distinguish two types of heat sources. One is the heat associated with the reversible cell reaction. The other is the irreversible heat, caused by the resistance to current passage. In conventional stacks, operating on externally reformed natural gas, significant removal of heat is necessary to maintain the stack temperature at about 650 °C.

There are conductive, convective and radiative heat-transfer phenomena between the fuel gas at the anode side compartment, electrodes with electrolyte matrix and oxidant gas at the cathode side compartment in the fuel cell. Furthermore, there is heat transfer due to mass transfer between the fuel gas and oxidant gas.

3. Related physical laws

The conservation laws of mass, energy and momentum are the basis of studying fuel cells [7]. Furthermore, electrochemical equations such as Nernst equation (Eq. (6)), give the electrical performance of fuel cells according to the energy conservation.

The terms in the following differential equations denote influences on a unit-volume basis. Thus:

$$\text{net efflux per unit volume} = \text{div } J = \frac{\partial J_x}{\partial x} + \frac{\partial J_y}{\partial y} + \frac{\partial J_z}{\partial z}$$

$$(8)$$

3.1. Conservation of a chemical species

Let m_1 denote the mass fraction of a chemical species. In the presence of a velocity field u, the conservation of m_1 is expressed as:

$$\frac{\partial}{\partial t} (\rho m_1) + \text{div}(\rho u m_1 + J_1) = R_1 \qquad (9)$$

Here $\partial(\rho m_1)/\partial t$ denotes the rate of change of the mass of the chemical species per unit volume. The quantity $\rho u m_1$ is the convection flux of the species, i.e., the flux carried by the general flow field ρu. The symbol J_1 stands for the diffusion flux, which is normally caused

by the gradients of m_1. The quantity R_1 on the right-hand side is the rate of generation of the chemical species per unit volume. This generation is caused by the chemical reaction.

3.2. Energy equation

The energy equation can be written as:

$$\frac{\partial(\rho h)}{\partial t} + \text{div}\left(\rho u h - \frac{k \nabla h}{C_p}\right) = S_h \qquad (10)$$

where h is the specific enthalpy, k the thermal conductivity, and S_h the volumetric rate of heat generation.

3.3. Momentum equation

The differential equation governing the conservation of momentum in a given direction for a newtonian fluid and laminar flow, which are assumed in this paper, can be written as:

$$\frac{\partial(\rho u)}{\partial t} + \text{div}(\rho u u - \mu \nabla u) = -\frac{\partial p}{\partial x} \qquad (11)$$

where μ is the viscosity, and p the pressure.

4. Computational fluid dynamic approach

The software package PHOENICS provides a solver for fluid-flow, heat-transfer, chemical-reaction and related problems ranging in complexity from one-dimensional single phase and steady state, to three-dimensional multi phase and transient. PHOENICS is used here to solve the three-dimensional conservation equations (Eqs. 8 to 11), which have been described in the former sections, in finite-volume form. All these conservation equations can be expressed in a single form:

$$\frac{\partial}{\partial t} (\rho \phi) + \text{div}(\rho V \phi - \Gamma_\phi \text{grad } \phi) = S_\phi \qquad (12)$$

where Γ_ϕ is the diffusion coefficient, S_ϕ the source term, and ϕ stands for any one of the dependent quantities: m_1, h, u or l. When $\phi = 1$, Eq. (12) turns to be a continuity equation.

To close the equations for a unique solution, boundary conditions must be provided. A universal formula can be used to describe all kinds of boundary conditions encountered in a fuel cell as a source term in Eq. (12).

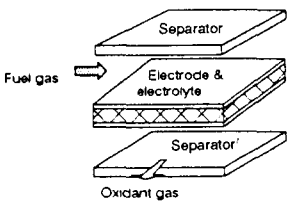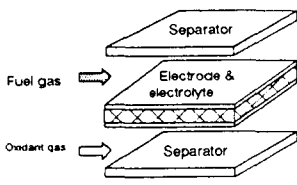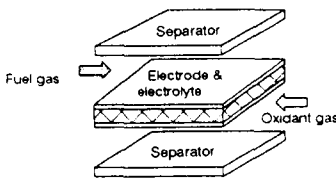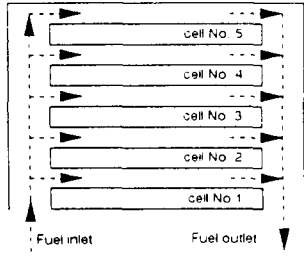$$S_\phi = [C_\phi + C_{mass}(V_{mass} - P)](V_\phi - \phi) \qquad (13)$$

where C_ϕ and V_ϕ are the 'coefficient' and the 'value', which are prescribed separately for each variable. V_{mass} has the physical significance of an external pressure, and the coefficient C_{mass}, that of the reciprocal of a flow resistance between the internal grid node, where

the pressure is p, and the external pressure is V_{mass} [6]. In this study, several separated sub-routines have been developed for the implementation of the chemical reaction, voltage–current relation and physical properties of gas and fuel-cell hardware. The fuel-cell modelling has been performed using PHOENICS version 1.6.6 on Convex 3840, and the following demonstrations were conducted.

5. Setting-up cases

To evaluate the present fuel-cell model, four cases listed in Table 1 were selected as examples for demonstration. The first three cell cases are used to illustrate the three-dimensional distributions of temperature, pressure, concentration and density across fuel cells

Table 1
Main features of the four cases

	Objectives of demonstration
Cell with cross flow	Temperature profiles across the cell at full and part electrical load
Cell with coflow	Distribution of temperature, pressure, concentration and density along the cell direction
Cell with counter flow	Distribution of temperature and pressure along the cell direction
Stack with cross flow	Temperature distribution across stack and mass distribution along the stack direction

with three different manifolds. By checking the behaviour of these distributions, the performance of the model dealing with the fundamental processes can be examined. Then, the stack case is set up to calculate temperature performance and mass distribution across the stack.

These four cases are assumed and characterized by the following specifications.

- Each cell has an electrochemical active area of 1 m×1 m and a thickness of 0.014 m surrounded by a frame of 20 mm containing the internal gas manifold.
- The stack contains 5 cross-flow cells. The inlet and the outlet of the fuel and oxidant gases are located at the bottom of the stack. This means that the fuel or oxidant gas first goes along the stack direction within the inlet manifolds, then turns along the cell flow path, and finally leaves downwards the stack via the outlet manifolds.
- The fuel gas uses Dutch natural gas (a mixture gas of H_2, CH_4, N_2, O_2, CO, CO_2, H_2O) which is supplied to the anode from the external reformer [8], and the oxidant gas uses a mixture gas of air and CO_2 which is supplied to the cathode.
- The inlet temperature of fuel and oxidant gas is 600 °C, and the outlet is at atmosphere pressure. Both the fuel and oxidant gases are considered as ideal.
- The operation of cell at constant voltage is also imposed, and average current density is set.
- The criteria for safe cell or stack operation here only monitor its temperature and pressure performance. That is, severe operational conditions only indicate high or high gradient of temperature on cell or stack hardware, and/or high pressure difference between fuel and oxidant gases.

6. Results and discussion

The results of the four cases will be discussed in the following sections. The height of cell or stack has been enlarged by a scale of 20:1.

6.1. Distributions of main parameters across fuel cells

6.1.1. Temperature distribution with cross-flow

In this Section we will examine the temperature distributions in the fuel cell, which can effectively illustrate the basic features of the operational performance. The following three factors have a contribution to the temperature distribution.

(i) reversible heat generated from chemical reactions;

(ii) irreversible heat generated from electrical resistance, and

(iii) heat transfer to the surroundings.

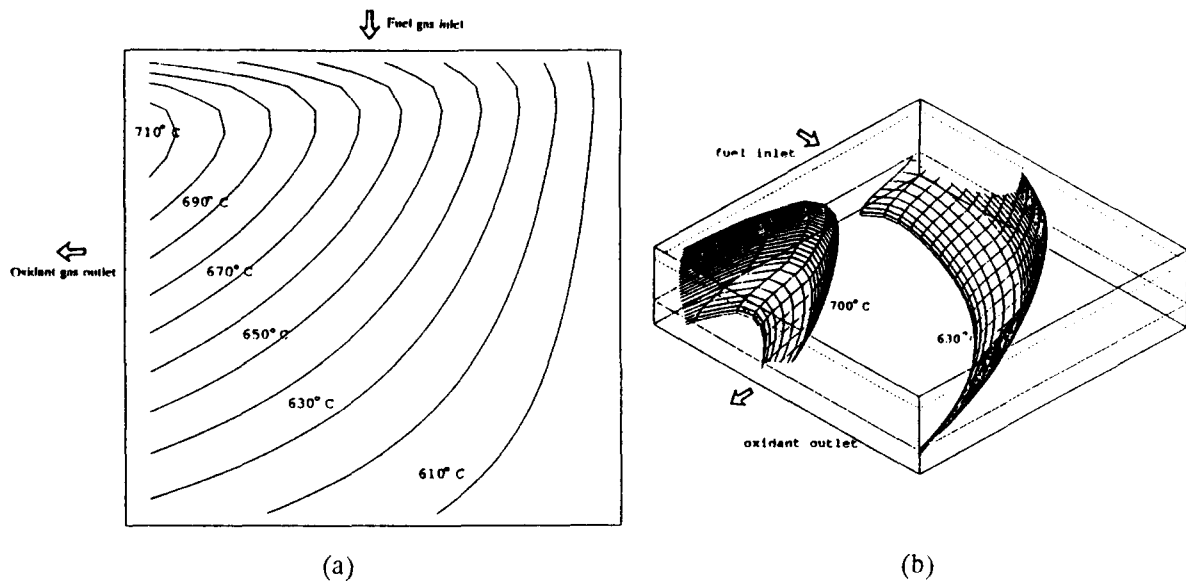The temperature profile of the cell with cross-flow operating at an average current of 1500 and 750

Fig. 2. Temperature profile of a cross-flow cell at an average current density 1500 A/m² (a) temperature at a transverse section of cell hardware, and (b) isothermal surface of temperature 700 and 630 °C.
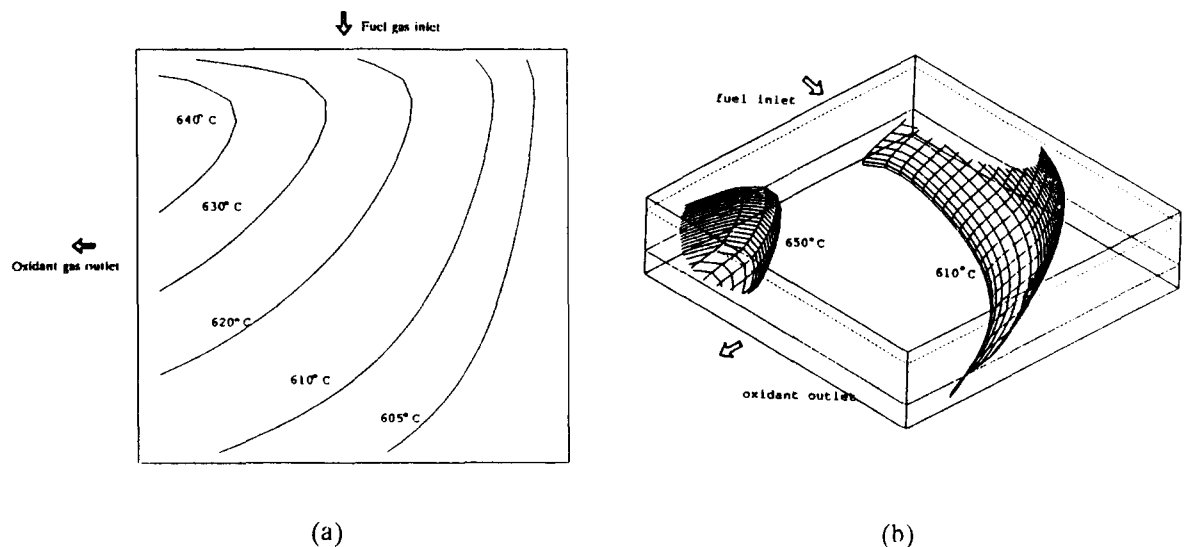

Fig. 3. Temperature profile of a cross-flow cell at an average current density of 750 A/m² (a) temperature distribution at a transverse section of cell hardware, and (b) isothermal surface of temperature 650 and 610 °C.

A/m² are shown in Figs. 2 and 3. The main features may be identified as follows.

• The point of maximum temperature is at 710 °C and is approximately located at the oxidant gas outlet and near the fuel gas inlet. This may be analysed qualitatively using the three factors given above. The first reversible heat from the chemical reactions at this location is high, since the fuel gas is relatively concentrated. The fuel gas utilization is much higher than that of the oxidant, which implies that the chemical reaction rate is more dependent on fuel gas composition than that of oxidant. The second factor, irreversible heat from the electrical resistance, is determined by the current and electrical resistance according to Ohm's

law. The third factor results in a higher temperature, since the oxidant gas at this location has been heated as it passes the cell.

• As expected, the maximum temperature and the temperature gradient of cells operating at a current density of 1500 A/m² is much higher than at 750 A/ m². Hence, a more severe temperature distribution appears at high current density.

6.1.2. Operational characteristics with co-flow

The distributions of temperature, pressure, density and gas composition for co-flow cells operating at an average current density of 1500 A/m² are discussed below. The corresponding results are shown in Fig. 4.
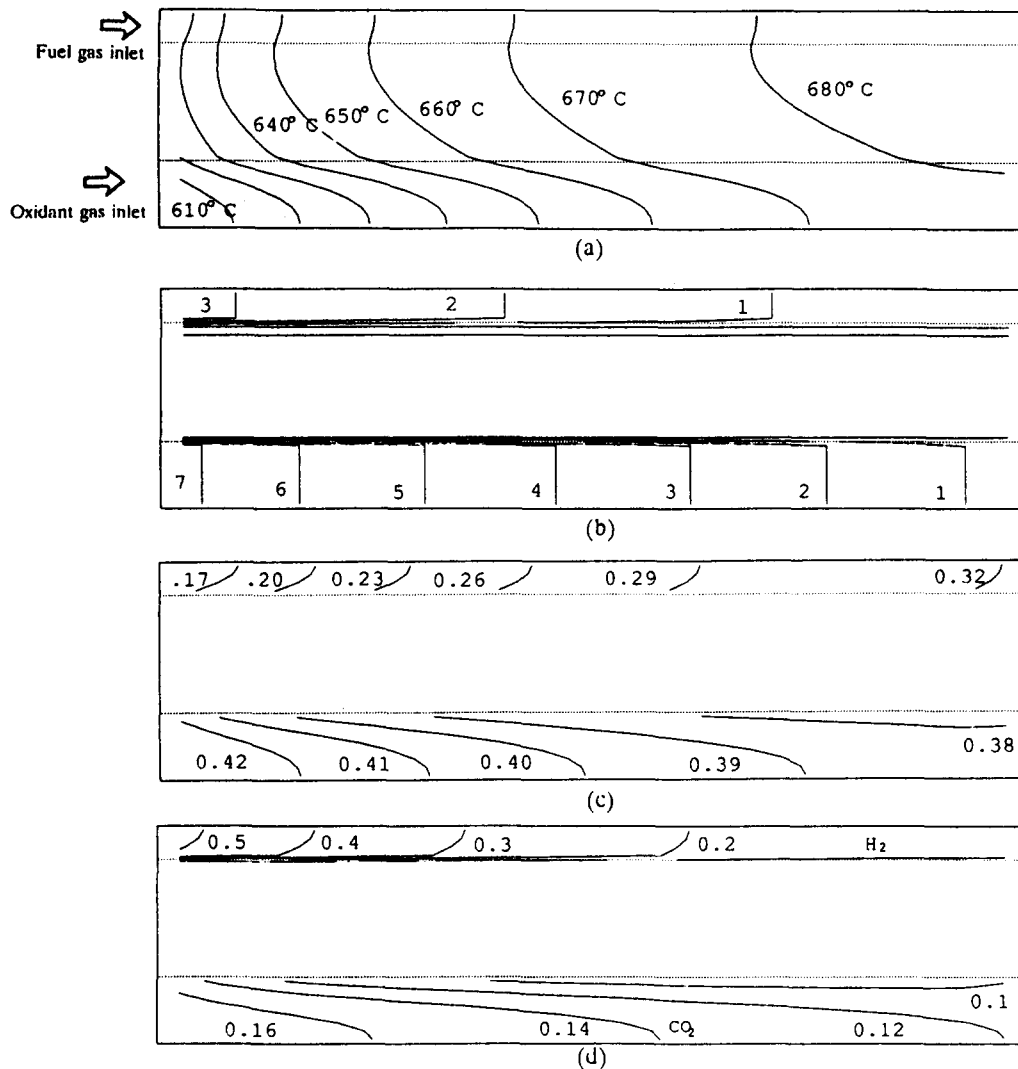
Fig. 4. Performance of a co-flow cell at an average current density of 1500 A/m^2: (a) temperature; (b) pressure (Pa); (c) H$_2$ and CO$_2$ concentration (mol/mol), and (d) gas density (kg/m^3).

The main characteristics can be summarized as follows.

● The temperatures of gases and cell hardware increase in the direction of gas flow, and the increment is larger near the gas inlet. This is the result of the heat generated from the chemical reactions and from the electrical resistance. In this case, the point of maximum temperature is at 680 °C, and is located around the anode gas outlet. However, the highest temperature gradient is near the inlet between the cathode gas and electrode.

● The pressure of fuel and oxidant gas decreases in the direction of the gas flow as expected. The highest pressure difference is 4 Pa, which occurs between the inlet of the anode and cathode gases. It is not large because the point of maximum pressure at the anode corresponds to the point of maximum pressure at the cathode.

● As expected, H$_2$ at the anode and CO$_2$ at the cathode decrease in the direction of gas flow, and the

decrease being more rapid near the inlet of the gas. This implies a greater rate of chemical reaction in the incoming gas than in the depleted gas.

● The density of the anode gas significantly increases and the density of the cathode gas decreases, in the direction of gas flow. In this case, the density of the anode gas at the inlet is lower than 0.17 kg/m^3 and at the outlet is greater than 0.32 kg/m^3, while the density of the cathode gas at the inlet is greater than 0.42 kg/m^3 and at the outlet it is lower than 0.38 kg/m^3. The change of gas density results from three factors: composition, temperature, and pressure changes. A greater percentage of the gas has heavier molecules, and is at a lower temperature and a higher pressure, resulting in a higher density. The considerable change in gas density shows the usual assumptions of constant gas density in the most of present modelling at the cell or stack level is unrealistic.
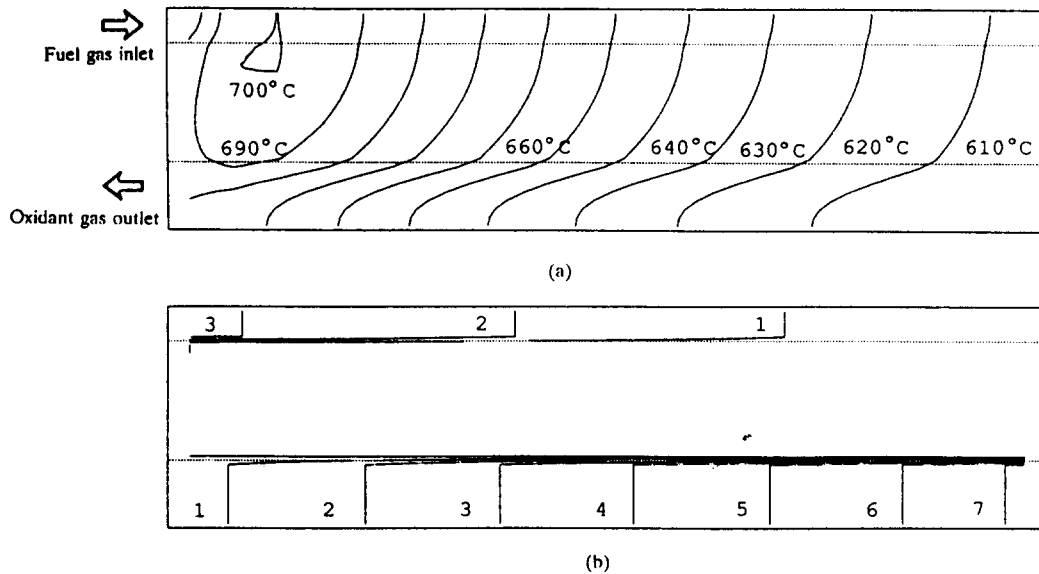
Fig. 5. Temperature profile of a counter-flow cell at an average current density of 1500 A/m² (a) temperature, and (b) pressure (Pa).

Table 2
Performance of cells with three different manifolds

	Maximum temperature and its location	Largest pressure difference and its location
Cross flow	710 °C, at the oxidant gas outlet and near the fuel gas inlet	6 Pa, near the oxidant inlet and the fuel gas outlet (not shown)
Coflow	680 °C, around the fuel gas outlet	4 Pa, between the fuel and oxidant gas inlets
Counter flow	700 °C, near the fuel gas inlet	7 Pa, between the fuel outlet and oxidant gas inlet

6.1.3. Temperature and pressure performance of a fuel cell with counter flow

The temperature and pressure distributions for a counter flow cell operating at an average current density of 1500 A/m² are illustrated in Fig. 5. The main characteristics may be identified as follows.

● The point of maximum cell temperature is 700 °C, located near the inlet of the anode gas. The temperature gradient is more uniform than that of the co-flow cell.

● The highest pressure difference is 7 Pa, which occurs between the fuel gas outlet and the oxidant gas inlet.

6.2. Comparison of fuel cells with different manifolds

A comparison of fuel cell types may be carried out in various ways, depending on use requirements. Here, one example is given to illustrate the effectiveness of the model in this application.

To determine the features for safe and efficient operation of fuel cells, the maximum temperature of

the fuel-cell hardware and the largest pressure difference between fuel and oxidant gases are often considered to be the two most important criteria. Accordingly, the characteristics of temperature and pressure difference for fuel cells with different manifolds described in the previous section are summarized in Table 2. The results indicate that the highest temperature appears in the cross-flow case, and the largest pressure difference appears in the counter-flow case.

6.3. Performance across the fuel-cell stack

With the model described, the three-dimensional distribution of operating parameters across a stack may be obtained. Below, temperature profiles and mass distributions are calculated to demonstrate the usefulness of the model as a study tool.

The temperature distributions in a transverse section of the oxidant gas outlet and the fuel gas outlet is shown in Fig. 6, at an average current density of 1500 A/m². The result indicates that the highest temperature is located at the top cell.

Mass flow along the vertical stack direction is one of the key parameters in the stack model, since it is closely related to inhomogeneous performance among different cells, which may influence the safe and efficient operation of a stack. Fig. 7 shows the fuel gas flow distribution along the stack direction with a cross-flow configuration at an average current density of 0, 750 and 1500 A/m².

When no current is drawn from the fuel-cell stack, the mass-transport processes can be modelled as a network of hydraulic resistances [9]. Thus, higher cells
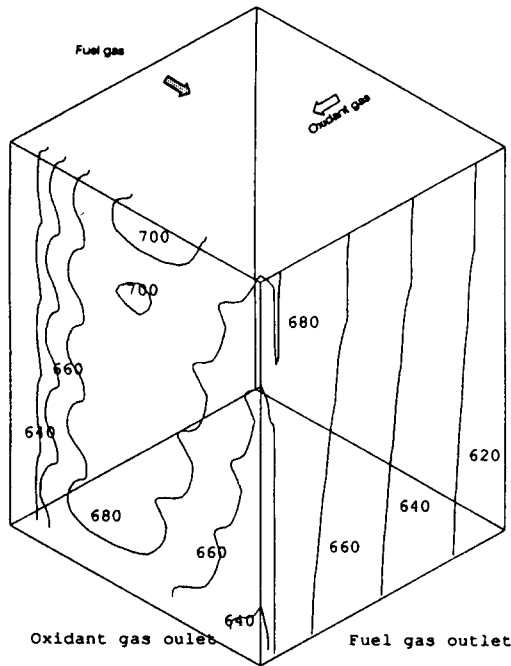
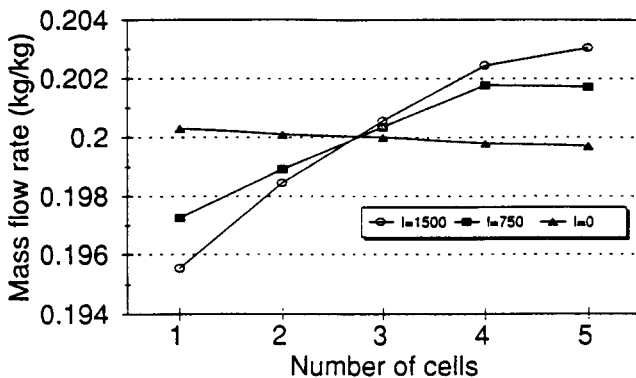Fig. 6. Temperature profile of a cross-flow stack of a current density 1500 A/m².

Fig. 7. Fuel gas distribution along the fuel stack direction; current density = 0, 750 and 1500 A/m².

(No. 5 being the top cell) in Fig. 7 have less fuel gas. However, when the current is drawn from the fuel-cell stack, the higher cells have more fuel gas. This may be interpreted due to the significant change in fuel-gas density (see Fig. 4(d)). However, this requires further confirmation. From the above results, it is clear that

the model presented here is capable of calculating the mass distribution along the stack direction.

7. Conclusions

A numerical model using the CFD technique for analysing MCFC performance is presented. The model considers the major factors which concern safe and efficient electricity generation. It has been applied to study the three-dimensional distributions of temperature, pressure, gas concentration, and density across fuel cells with different manifolds. The results appear to be reasonable. Moreover, the model has demonstrated features which may be used to optimize the design and to analyse the operation of fuel cell stacks.

The conclusions only apply to internal manifolding. External manifolding may be different, e.g. in the cross-flows case.

Acknowledgements

References

[1] International Energy Agency, SOFC stack design tool, Final Rep., Swiss Federal Office of Energy, Berne, Nov. 1992.
[2] G.K. Troost, J. Power Sources, 49 (1994) 185–192.
[3] T.L. Wolf and G. Wilemski, J. Electrochem. Soc., 130 (1983) 48–55.
[4] E. Achenbach, J. Power Sources, 49 (1994) 333–348.
[5] S. Takashima, MCFC stack modelling and test at Hitachi, Workshop Molten Carbonate Fuel Cells Systems, British Gas, 27 Sept. 1993, Loughborough, UK, unpublished.
[6] CHAM Development Team, The PHOENICS Reference Manual, TR200', Concentration, Heat and Mometum Limited, London, 1991.
[7] S.V. Patankar, Numerical heat transfer and fluid flow, McGraw-Hill, New York, 1980.
[8] W. He, J. Power Sources, 49 (1994) 283–290.
[9] R.J. Boersma and L.A.H. Machielse, Distribution of glasflow in internally manifolded fuel cell stacks, Proc. Int. Fuel Cell Conf., Makuhari, Japan, 3–6 Feb. 1992, pp. 255–259.